

# Spin-Wave Theory of the Multiple-Spin Exchange Model on a Triangular Lattice in a Magnetic Field : 3-Sublattice Structures

CHITOSHI YASUDA\*, DAISUKE KINOUCI and KENN KUBO

*Department of Physics and Mathematics, Aoyama Gakuin University, Sagami-hara 229-8558, Japan*

We study the spin wave in the  $S = 1/2$  multiple-spin exchange model on a triangular lattice in a magnetic field within the linear spin-wave theory. We take only two-, three- and four-spin exchange interactions into account and restrict ourselves to the region where a coplanar three-sublattice state is the mean-field ground state. We found that the Y-shape ground state survives quantum fluctuations and the phase transition to a phase with a 6-sublattice structure occurs with softening of the spin wave. We estimated the quantum corrections to the ground state sublattice magnetizations due to zero-point spin-wave fluctuations.

**KEYWORDS:** multiple-spin exchange model, three-sublattice structure, spin-wave approximation, softening, sublattice magnetization, quantum phase transition, solid helium, frustration

## 1. Introduction

The multiple-spin exchange (MSE) model on the triangular lattice is one of the two dimensional frustrated quantum spin systems which are presently at the focus of strong interest. The model is believed to describe nuclear magnetism of the solid  $^3\text{He}$  layers adsorbed on graphite,<sup>1-3</sup> whose peculiar temperature dependence of the specific heat with a double-peaked structure is quite intriguing.<sup>4</sup> Several studies were devoted for theoretical understanding of the experimental results in terms of the MSE model.<sup>5-13</sup> The mean-field theory was applied to the MSE model with two-, three- and four-spin cyclic exchange interactions, which lead to various kinds of the ground state corresponding to different values of parameters.<sup>5,13</sup> Appearance of various mean-field ground states reflects weak stability of the mean-field ground states due to strong frustration. Therefore quantum fluctuations should have strong influence on the ground state of the system. Quantum mechanical ground state was studied by the numerical diagonalization of finite clusters and a spin liquid ground state with a finite spin gap was predicted for the parameters which are thought to be adequate to the  $^3\text{He}$  layer.<sup>9,10</sup> However recent measurement of the susceptibility down to  $\sim 10 \mu\text{K}$  did not show any sign which suggests the existence of a spin gap.<sup>14</sup> At present, the ground state of both the two-dimensional solid  $^3\text{He}$  on graphite and the MSE model on the triangular lattice are, therefore, hardly understood. The MSE interactions might be relevant as well to the spin liquid state of  $\kappa\text{-(ET)}_2\text{Cu}_2(\text{CN})_3$  where antiferromagnetic interaction is thought to be dominant.<sup>15</sup> Therefore it is meaningful and desired to study the properties of the MSE model on the triangular lattice into detail.

In the present work, we study the spin wave in the  $S = 1/2$  MSE model with two-, three- and four-spin exchange interactions on the triangular lattice in the magnetic field. The system is described by the Hamiltonian

$$\mathcal{H} = J \sum_{\langle i,j \rangle} \boldsymbol{\sigma}_i \cdot \boldsymbol{\sigma}_j + K \sum_{\text{p}} h_{\text{p}} + h \sum_i \sigma_i^z, \quad (1)$$

where  $\boldsymbol{\sigma}_i$  is the Pauli matrix on the site  $i$  and the summations  $\sum_{\langle i,j \rangle}$  and  $\sum_{\text{p}}$  run over all pairs and minimum diamonds, respectively. Since the three-spin exchange interaction is reduced to the conventional two-spin one, the first term of the Hamiltonian (1) describes the sum of two- and three-spin exchange interactions. The Hamiltonian  $h_{\text{p}}$  is the four-spin exchange interaction for a minimum diamond  $\text{p}$ . For a diamond of spins  $1 \sim 4$  with diagonal bonds (1,3) and (2,4), it reads

$$\begin{aligned} h_{\text{p}} = & \sum_{1 \leq i < j \leq 4} \boldsymbol{\sigma}_i \cdot \boldsymbol{\sigma}_j + (\boldsymbol{\sigma}_1 \cdot \boldsymbol{\sigma}_2)(\boldsymbol{\sigma}_3 \cdot \boldsymbol{\sigma}_4) \\ & + (\boldsymbol{\sigma}_1 \cdot \boldsymbol{\sigma}_4)(\boldsymbol{\sigma}_2 \cdot \boldsymbol{\sigma}_3) - (\boldsymbol{\sigma}_1 \cdot \boldsymbol{\sigma}_3)(\boldsymbol{\sigma}_2 \cdot \boldsymbol{\sigma}_4). \quad (2) \end{aligned}$$

The coupling parameters are written in terms of conventional exchange constants as  $K = -J_4/4$  and  $J = J_3 - J_2/2$ . Since  $J_n$  are known to be negative in solid  $^3\text{He}$ ,<sup>16</sup> we take the value of  $K$  positive in the following. The third term in Eq. (1) is the Zeeman term with a magnetic field  $\mathbf{h}$  ( $h = |\mathbf{h}|$ ) applied anti-parallel to the  $z$ -direction as shown in Fig. 1.

Numerous mean-field ground-state phases were found for the Hamiltonian (1) by assuming up to 144 sublattices.<sup>13</sup> The phase diagram is parametrized by  $J/K$  and  $h/K$ . When  $h = 0$ , the ground state varies according to  $J/K$  as follows : I) the ferromagnetic phase for  $J/K < -8.61$ . II) the intermediate phase for  $-8.61 < J/K < -2.26$  where the ground state spin structure varies with the change of  $J/K$  and ten small phases with equal to or more than 12 sublattices were identified. These small phases might be artifacts of assumptions of finite number of sublattices. The true ground state in this parameter region is still controversial even at the mean-field level. III) the tetrahedral phase for  $-2.26 < J/K < 8.22$ . The ground state has a 4-sublattice spin structure with zero magnetization, where spin vectors on four sublattices point four vertices of a tetrahedron if their bottoms are put at its center. IV) a phase with six sublattices for  $8.22 < J/K < 10$ . The ground state has non-coplanar spin structure with uniform vector chiral order and staggered scalar chiral order. Finally, V) the  $120^\circ$  phase for

\*E-mail address: cvasuda@phvs.aoyama.ac.jp

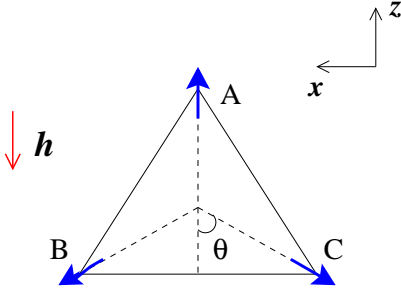


Fig. 1. Y-shape state on a triangular lattice in a magnetic field  $h$ .

$J > 10K$ . The spins on three sublattices make the angle  $2\pi/3$  to each other.

The mean-field phase diagram in the magnetic field was also studied.<sup>5,12,13</sup> One of the interesting behaviors is the appearance of a magnetization plateau with  $1/2$  of the full polarization in the parameter region adequate to  $^3\text{He}$  layers.<sup>5,9,12</sup> This plateau is realized by the 4-sublattice uud spin structure. Other numerous ground-state phases in the magnetic field have been found, but we introduce only the phases related to the present work. The  $120^\circ$  ground state for  $J > 10K$  is modified by the magnetic field. This state has a 3-sublattice coplanar spin configuration with the spins on one (say A) sublattice antiparallel to the applied magnetic field. The spins on other sublattices (B and C) tilt toward the oblique directions as shown in Fig. 1. In the present paper, we call it Y-shape state.<sup>17</sup> This result shows that the four-spin exchange interaction lifts the non-trivial degeneracy of the mean-field ground-state of the antiferromagnetic Heisenberg (AFH) model in the magnetic field.<sup>18</sup> A 6-sublattice phase exists for  $8 \lesssim J/K \lesssim 10$  adjacent to the Y-shape state for weak magnetic field. Increase in the magnetic field induces a 12-sublattice structure. Further increase in the magnetic field leads to a magnetization plateau with  $1/3$  of full polarization due to the 3-sublattice uud state with two sublattices with up spins and the other with down spins. The uud state is stabilized by the four-spin interaction and occupies a large region in the phase diagram. We note that the phase boundary between the Y-shape and the 6-sublattice phases was not determined by the mean-field theory.

Spin waves in this model were studied previously in the absence of the magnetic field.<sup>6,7,12</sup> The spin wave in the tetrahedral phase was studied and the quantum corrections to the sublattice magnetization were estimated.<sup>6</sup> The analysis for  $J = 0$  showed the stability of the tetrahedral state against the zero-point fluctuations of the spin wave. The spin wave in the  $120^\circ$  phase was studied and it was shown that there are three gapless branches for small  $k$  and the spin wave softens at  $J = 10K$ .<sup>7</sup> The softening corresponds to the phase transition to the 6-sublattice phase.

In the present work, we investigate the spin wave in the Y-shape phase and discuss the phase transition under the magnetic field. Although the Y-shape phase does not correspond to the model for the solid  $^3\text{He}$  layer,<sup>19</sup> coplay

of the geometrical frustration and the MSE interactions poses a problem of interest in itself. We investigated the dispersions of the spin waves as well as the effects of the zero-point fluctuations of the spin wave on the ground-state energies. As a result, we found that though the Y-shape ground state survives quantum fluctuations for  $J/K \gtrsim 12$  and small  $h/K$ , softening of the spin wave leads to the phase transition to the 6-sublattice phase.

The present paper is organized as follows. In § 2, we present the linear spin-wave theory for the Y-shape state in the magnetic field. In § 3, we simply summarize the magnetic properties in two special cases, i.e., the AFH model in the magnetic field and the MSE model at  $h = 0$ . The dispersion of the spin wave and the phase diagram obtained from the softening of the spin wave are shown in § 4 and 5, respectively. The quantum effects are discussed by studying quantum corrections of the ground-state energy and the sublattice magnetizations in § 6. Finally, § 7 is devoted to summary and discussion.

## 2. Spin-Wave Theory for the Y-Shape State

Assuming the Y-shape state as the ground state, we can perform the Holstein-Primakoff transformation<sup>20</sup> of the Hamiltonian (1) by neglecting higher-order terms as

$$\begin{cases} \sigma_i^z \simeq 1 - 2a_i^\dagger a_i \\ \sigma_i^+ \simeq a_i \\ \sigma_i^- \simeq a_i^\dagger \end{cases}, \quad (3)$$

for  $i \in \text{A sublattice}$ ,

$$\begin{cases} \sigma_j^z \simeq -\alpha(b_j^\dagger + b_j) - \beta(1 - 2b_j^\dagger b_j) \\ \sigma_j^+ \simeq \frac{1}{2}\{\alpha(1 - 2b_j^\dagger b_j) - (\beta + 1)b_j^\dagger - (\beta - 1)b_j\} \\ \sigma_j^- \simeq \frac{1}{2}\{\alpha(1 - 2b_j^\dagger b_j) - (\beta - 1)b_j^\dagger - (\beta + 1)b_j\} \end{cases}, \quad (4)$$

for  $j \in \text{B sublattice}$ , and

$$\begin{cases} \sigma_k^z \simeq \alpha(c_k^\dagger + c_k) - \beta(1 - 2c_k^\dagger c_k) \\ \sigma_k^+ \simeq \frac{1}{2}\{-\alpha(1 - 2c_k^\dagger c_k) - (\beta + 1)c_k^\dagger - (\beta - 1)c_k\} \\ \sigma_k^- \simeq \frac{1}{2}\{-\alpha(1 - 2c_k^\dagger c_k) - (\beta - 1)c_k^\dagger - (\beta + 1)c_k\} \end{cases}, \quad (5)$$

for  $k \in \text{C sublattice}$ , where  $a_i^\dagger$  ( $a_i$ ),  $b_j^\dagger$  ( $b_j$ ) and  $c_k^\dagger$  ( $c_k$ ) are the boson creation (annihilation) operators,  $\alpha = \sin \theta$  and  $\beta = \cos \theta$  as shown in Fig. 1.

First, we obtain the relation between  $h$  and the angle  $\theta$  from the condition that the first-order terms of the transformed Hamiltonian should vanish, i.e.,

$$\cos \theta = \frac{1}{12K} \{5K + J - \sqrt{(J - K)^2 - 4Kh}\}, \quad (6)$$

for  $h \leq h_c$  where

$$h_c = -12K + 3J. \quad (7)$$

The value of  $\theta$  monotonously decreases with the increase of  $h$  and the uud state ( $\theta = 0$ ) is realized for  $h \geq h_c$ . This relation can be also obtained from  $dE^{\text{cl}}/d\theta = 0$  where the mean-field ground-state energy  $E^{\text{cl}}$  per the total number of sites  $N$  is given by

$$\begin{aligned} E^{\text{cl}}/N &= (2\beta^2 - 2\beta - 1)J \\ &\quad - (8\beta^3 - 10\beta^2 + 4\beta + 1)K + \frac{1}{3}(1 - 2\beta)h. \end{aligned} \quad (8)$$

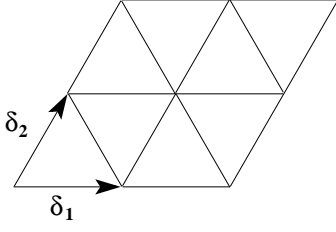


Fig. 2. Unit vectors  $\delta_1 = (1, 0)$  and  $\delta_2 = (0, 1)$  on the triangular lattice.

After straightforward calculations the Hamiltonian is rewritten as

$$\mathcal{H} = E^{\text{cl}} + \sum_{\mathbf{k}} \mathbf{v}_{\mathbf{k}}^\dagger \mathcal{D} \mathbf{v}_{\mathbf{k}} + E_0^{\text{q}}, \quad (9)$$

where  $\mathbf{v}_{\mathbf{k}}^\dagger = (a_{\mathbf{k}}^\dagger, b_{\mathbf{k}}^\dagger, c_{\mathbf{k}}^\dagger, a_{-\mathbf{k}}, b_{-\mathbf{k}}, c_{-\mathbf{k}})$  and  $\sum_{\mathbf{k}}$  in the second term denotes the summation over a half of the reduced Brillouin zone of the 3-sublattice structure. The matrix  $\mathcal{D}$  reads

$$\mathcal{D} = \begin{pmatrix} M_{\text{diag}} & M_{\text{off}} \\ M_{\text{off}} & M_{\text{diag}} \end{pmatrix}, \quad (10)$$

where

$$M_{\text{diag}} = \begin{pmatrix} A_{\mathbf{k}} & C\Gamma_{\mathbf{k}} & C\Gamma_{\mathbf{k}}^* \\ C\Gamma_{\mathbf{k}}^* & B_{\mathbf{k}} & D\Gamma_{\mathbf{k}} \\ C\Gamma_{\mathbf{k}} & D\Gamma_{\mathbf{k}}^* & B_{\mathbf{k}} \end{pmatrix}, \quad (11)$$

and

$$M_{\text{off}} = \begin{pmatrix} E_{\mathbf{k}} & G\Gamma_{\mathbf{k}} & G\Gamma_{\mathbf{k}}^* \\ G\Gamma_{\mathbf{k}}^* & F_{\mathbf{k}} & H\Gamma_{\mathbf{k}} \\ G\Gamma_{\mathbf{k}} & H\Gamma_{\mathbf{k}}^* & F_{\mathbf{k}} \end{pmatrix}, \quad (12)$$

with

$$\begin{aligned} A_{\mathbf{k}} &= 12\{-2K + (J + 2K)\beta + 4K\beta^3 \\ &\quad + K(1 - \beta^2)\Delta_{\mathbf{k}}\} - 2h, \\ B_{\mathbf{k}} &= 6\{J + 2K + (J - 4K)\beta - 2(J + 5K)\beta^2 \\ &\quad + 12K\beta^3 + 2K(1 - \beta + 2\beta^3)\Delta_{\mathbf{k}}\} + 2h\beta, \\ C &= 3(1 - \beta)(J + 4K + 4K\beta^2), \\ D &= 6\{K(4\beta - 1) + (J + 5K)\beta^2 - 8\beta^3 K\}, \\ E_{\mathbf{k}} &= -12(1 - \beta^2)K\Delta_{\mathbf{k}}, \\ F_{\mathbf{k}} &= 2\beta E_{\mathbf{k}}, \\ G &= -3(1 + \beta)(J + 4\beta^2 K), \\ H &= -6(1 - \beta^2)(J + 5K - 8\beta K). \end{aligned} \quad (13)$$

Here the wave-number dependence is incorporated by

$$\Gamma_{\mathbf{k}} = \frac{1}{3}(e^{ik_1} + e^{-ik_2} + e^{i(-k_1+k_2)}), \quad (14)$$

$$\Delta_{\mathbf{k}} = \frac{1}{3}\{\cos(k_1 + k_2) + \cos(2k_1 - k_2) + \cos(-k_1 + 2k_2)\}, \quad (15)$$

where  $k_i = \mathbf{k} \cdot \delta_i$   $i = 1, 2$  is an element of the wave vector and the unit vector  $\delta_1$  and  $\delta_2$  of the triangular lattice

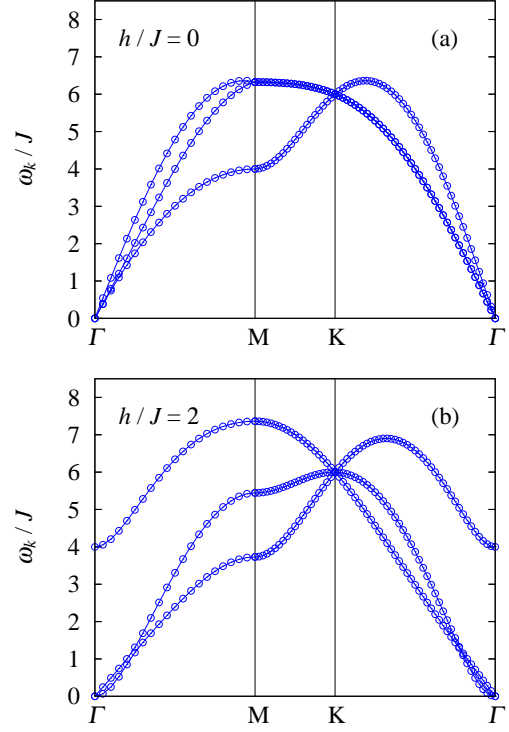


Fig. 3. Three dispersions of the spin wave for the AFH model with (a)  $h = 0$  and (b)  $h/J = 2$ . The marks  $\Gamma$ ,  $M$  and  $K$  denote the wave numbers as defined in Fig. 4 and the vertical axis the lines  $\Gamma$ - $M$ - $K$ - $\Gamma$ .

are chosen as shown in Fig. 2. Note that  $k_1^2 + k_2^2 - k_1 k_2 = 3k^2/4$  holds. The third term in Eq. (9)

$$E_0^{\text{q}} = - \sum_{\mathbf{k}} (A_{\mathbf{k}} + 2B_{\mathbf{k}}) \quad (16)$$

arises from the Bose commutation relation. The Hamiltonian (9) is diagonalized through the Bogoliubov transformation and takes the following form:

$$\mathcal{H} = E^{\text{cl}} + \sum_{\mathbf{k}} \mathbf{u}_{\mathbf{k}}^\dagger \mathcal{D}_{\text{diag}} \mathbf{u}_{\mathbf{k}} + E_0^{\text{q}}, \quad (17)$$

where  $\mathbf{u}_{\mathbf{k}}^\dagger = (a_{\mathbf{k}}^\dagger, \beta_{\mathbf{k}}^\dagger, \gamma_{\mathbf{k}}^\dagger, \alpha_{-\mathbf{k}}, \beta_{-\mathbf{k}}, \gamma_{-\mathbf{k}})$  is a vector of the transformed Bose operators and  $\mathcal{D}_{\text{diag}}$  is a diagonal matrix whose  $(i, i)$  elements are  $\omega_{\mathbf{k}}^{(1)}, \omega_{\mathbf{k}}^{(2)}, \omega_{\mathbf{k}}^{(3)}, \omega_{\mathbf{k}}^{(1)}, \omega_{\mathbf{k}}^{(2)}$  and  $\omega_{\mathbf{k}}^{(3)}$  for  $i = 1 \sim 6$ . The frequencies of the three branches of the spin wave are given by  $\omega_{\mathbf{k}}^{(1)}, \omega_{\mathbf{k}}^{(2)}$  and  $\omega_{\mathbf{k}}^{(3)}$ . We numerically performed the transformation according to the general theory by Colpa.<sup>21</sup>

### 3. Spin-Wave Spectrum of the AFH Model in the Magnetic Field and the MSE Model at $h = 0$

In this section we reproduce the previously known results for simple cases in order for comparison with the results in the next section.

First we demonstrate the results for  $K = 0$ , i.e., the AFH model. The dispersions of the spin waves assuming the Y-shape state as the ground state for the AFH model with  $h/J = 0$  and 2 are shown in Figs. 3 (a)

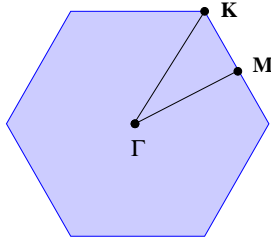


Fig. 4. Brillouin zone of the 3-sublattice structure with reciprocal lattice vectors  $(k_1, k_2) = (2\pi/3, -2\pi/3)$  and  $(2\pi/3, 4\pi/3)$ . The marks  $\Gamma$ , M and K denote  $(k_1, k_2) = (0,0)$ ,  $(2\pi/3, \pi/3)$  and  $(2\pi/3, 2\pi/3)$ , respectively.

and (b), respectively. The hexagonal Brillouin zone for the 3-sublattice structure is shown in Fig. 4. For  $h = 0$  the frequencies of all spin-wave branches vanish at the  $\Gamma$  point ( $\mathbf{k} = 0$ ) and have the linear dispersion for small  $k$ . In the magnetic field, one of the three branches is lifted to  $\omega_{\mathbf{k}} = 2h$  at the  $\Gamma$  point corresponding to the uniform precession of the spins about the magnetic field. There are two gapless branches rather than one expected from the  $SO(2)$  symmetry. Furthermore one of them has a quadratic dispersion for small  $k$ . This is caused by a non-trivial continuous degeneracy in the mean-field ground state in the magnetic field.<sup>18</sup> Any three-sublattice spin structure fulfilling the relation  $\mathbf{S}_A + \mathbf{S}_B + \mathbf{S}_C = \mathbf{h}/3J$  is a ground state for  $h \leq 3J$ , where  $\mathbf{S}_{A,B,C}$  is the sublattice magnetization on each sublattice. Chubukov and Golosov showed that quantum fluctuations lift this non-trivial degeneracy and select the coplanar spin structure, i.e., the Y-shape state.<sup>22</sup> This is an example of the so-called order from disorder phenomena.

Next we show the result for the MSE model at  $\mathbf{h} = 0$ . In this case the transformed Hamiltonian (9) can be analytically diagonalized<sup>7</sup> as

$$\mathcal{H} = E^{\text{cl}} + \sum_{\mathbf{k}} (\omega_{\mathbf{k}}^{(1)} \alpha_{\mathbf{k}}^\dagger \alpha_{\mathbf{k}} + \omega_{\mathbf{k}}^{(2)} \beta_{\mathbf{k}}^\dagger \beta_{\mathbf{k}} + \omega_{\mathbf{k}}^{(3)} \gamma_{\mathbf{k}}^\dagger \gamma_{\mathbf{k}}) + E^{\text{q}}, \quad (18)$$

where the summation of the second term runs over the Brillouin zone, and

$$\begin{aligned} \omega_{\mathbf{k}}^{(\mu)} &= \sqrt{V_{\mathbf{k}}^{(\mu)} - W_{\mathbf{k}}^{(\mu)}}, \\ V_{\mathbf{k}}^{(1)} &= 6(J - K) + 9K\Delta_{\mathbf{k}} + 3(J + 5K)\Gamma'_{\mathbf{k}}, \\ W_{\mathbf{k}}^{(1)} &= 9\{K\Delta_{\mathbf{k}} + (J + K)\Gamma'_{\mathbf{k}}\}, \end{aligned} \quad (19)$$

and  $\Gamma'_{\mathbf{k}} = \text{Re}(\Gamma_{\mathbf{k}})$ ,  $V_{\mathbf{k}}^{(2)} = V_{\mathbf{k}+\mathbf{Q}}^{(1)}$ ,  $W_{\mathbf{k}}^{(2)} = W_{\mathbf{k}+\mathbf{Q}}^{(1)}$ ,  $V_{\mathbf{k}}^{(3)} = V_{-\mathbf{k}+\mathbf{Q}}^{(1)}$ ,  $W_{\mathbf{k}}^{(3)} = W_{-\mathbf{k}+\mathbf{Q}}^{(1)}$  where  $\mathbf{Q} = (-2\pi/3, 2\pi/3)$ . The first and third terms of Eq. (18) are

$$E^{\text{cl}} = -\frac{3}{2}(J + K)N, \quad (20)$$

$$E^{\text{q}} = \frac{1}{2} \sum_{\mu=1}^3 \sum_{\mathbf{k}} (\omega_{\mathbf{k}}^{(\mu)} - V_{\mathbf{k}}^{(\mu)}). \quad (21)$$

We show the spin-wave spectrum for  $J/K = 12$  and 10 in Figs. 5 (a) and (b), respectively. The frequencies of branches vanish at the  $\Gamma$  point as for the AFH model.

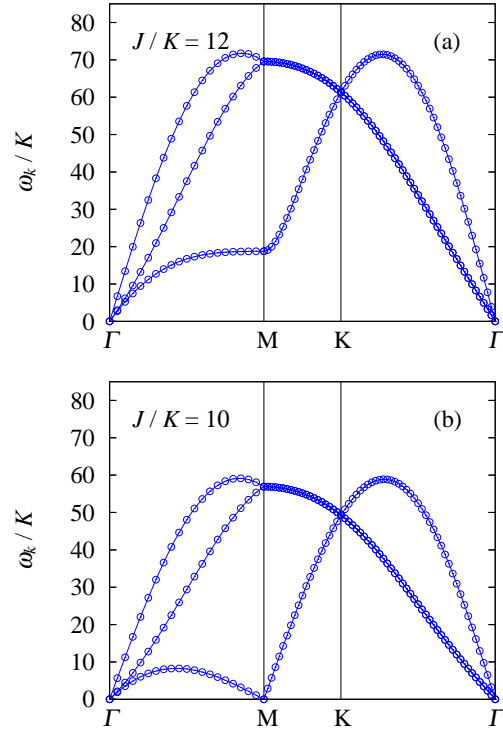


Fig. 5. Three dispersions of the spin wave for (a)  $J/K = 12$  and (b)  $J/K = 10$  at  $h = 0$ . The marks  $\Gamma$ , M and K denote the wave number vectors as shown in Fig. 4 and the vertical axis the lines  $\Gamma$ -M-K- $\Gamma$ .

They have linear dispersions for small  $k$  as

$$\omega_{\mathbf{k}}^{(1)} \simeq 3\sqrt{3(J - K)(J + 2K)} k, \quad (22)$$

$$\begin{aligned} \omega_{\mathbf{k}}^{(2)} &\simeq \omega_{\mathbf{k}}^{(3)} \\ &\simeq 3\sqrt{6(J - K)\{(J - 7K)(k_1^2 + k_2^2) - (J + 5K)k_1 k_2\}}. \end{aligned} \quad (23)$$

Figure 5 shows that the frequency of the second branch  $\omega_{\mathbf{k}}^{(2)}$  vanishes at the M point, which indicates that a second-order phase transition to the 6-sublattice structure occurs due to the softening of the spin wave just at  $J = 10K$ .<sup>7</sup> The softening occurs at six equivalent M points in the Brillouin zone.

#### 4. Spin-Wave Spectrum of the MSE Model in the Magnetic Field

In Figs. 6 (a) and (b) we show the dispersion for  $J/K = 12$  and 10.14 at  $h = 10K$ . In contrast with the spectrum in the AFH model, there is only one gapless branch at the  $\Gamma$  point and the gapless branch has a linear dispersion. The result is consistent with the excitations from a stable ground state only with the global  $SO(2)$  symmetry and corresponds to that the four-spin exchanges stabilize the coplanar Y-shape state already in the mean-field approximation. The frequency of the lowest branch decreases at the M point with decreasing  $J/K$  for a fixed  $h$ . It vanishes at a critical value of  $J/K$  as shown in Fig. 6 (b). The  $J/K$ -dependence of the frequency of the spin wave at the point M ( $\mathbf{k} = (2\pi/3, \pi/3)$ ) is shown in Fig. 7 for various values of  $h$ . The softening of the spin wave is induced by the competition of the two-

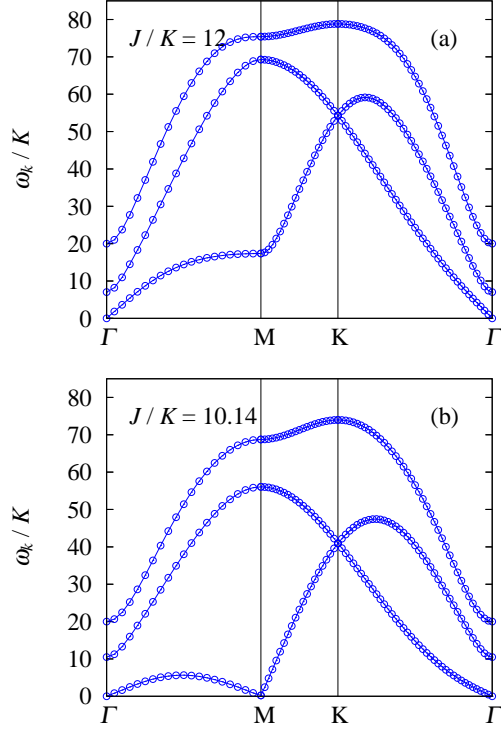


Fig. 6. Three dispersions of the spin wave for (a)  $J/K = 12$  and (b)  $J/K = 10.14$  at  $h/K = 10$ . The frequency of the lowest branch at the M point vanishes at  $J/K \simeq 10.14$ .

and four-spin interactions in the magnetic field. The frequency vanishes apparently as  $\omega_k \propto (J - J_c)^\beta$ . Here we assume the critical exponent  $\beta$  to be  $1/2$  which results from the general Landau theory. The softening of the spin wave leads to a phase transition to the 6-sublattice phase in the magnetic field. We determine the phase boundary between the Y-shape and the 6-sublattice phases by determining the critical value in the next section.

## 5. The Phase Diagram

In Fig. 8 we show the phase diagram determined from the softening of the spin wave together with the phase boundaries determined by the mean-field calculations. The phase boundary between the Y-shape and the 6-sublattice phases extends from  $(J/K, h/K) = (10, 0)$  to the multi-critical point  $((J/K)_{\text{multi}}, (h/K)_{\text{multi}})$  where four phase boundaries appear to merge. Phase transitions from the Y-shape phase to the 6-sublattice and the uud phases are continuous. On the other hand, the transition between the 6-sublattice and the 12-sublattice phases and that between the 12-sublattice and the uud phases are discontinuous. The phase boundary between the Y-shape and the uud phases is given by the relation (7) and the multi-critical point is estimated to be  $((J/K)_{\text{multi}}, (h/K)_{\text{multi}}) \simeq (11.37, 22.11)$ . Though in the AFH model the uud phase occurs only at a critical value  $h_c = 3J$  in the mean-field theory, the phase extends to a finite region of  $h$  in the MSE model. The four-spin exchange stabilizes the uud state. It was shown that the thermal or quantum fluctuations stabilize the uud state.<sup>18, 22</sup> The four-spin exchange has a same effect and as a result magnifies the  $1/3$  magnetization plateau.

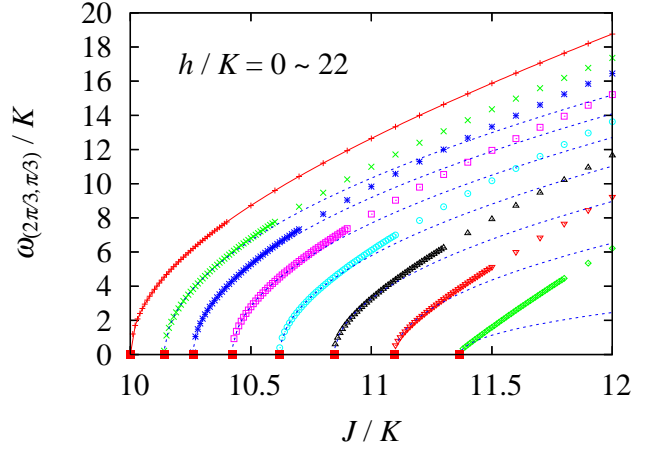


Fig. 7.  $J/K$ -dependences of the frequency of the spin wave at the point M in the magnetic field  $h/K = 0, 10, 12, 14, 16, 18, 20$  and  $22$  from top. The solid marks for  $\omega(2\pi/3, \pi/3) = 0$  denote the phase-transition points. The bold line for  $h/K = 0$  is analytically obtained by using Eq. (19). The broken lines are obtained by the least-squares fitting with the fitting function  $\omega_k \propto (J - J_c)^\beta$  with  $\beta = 1/2$ .

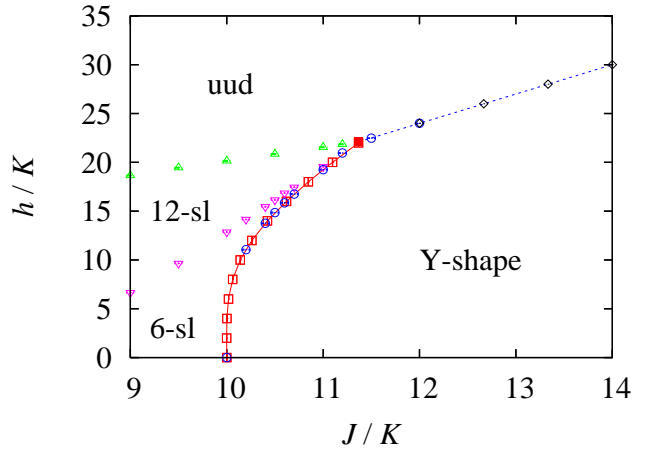


Fig. 8. Phase diagram parametrized by the two-spin interaction and the magnetic field. The abbreviations of Y-shape, 6-sl, 12-sl and uud denote the phases with the Y-shape, 6-, 12-sublattice and uud structures. The open squares are estimated by the softening of the spin wave at  $\mathbf{k} = (2\pi/3, \pi/3)$ . The diamonds denote the parameters at which the total magnetization is equal to the saturated value  $1/3$  of the uud structure. The broken line is the phase-transition line  $h_c = -12K + 3J$ . For reference, the data in ref. 13 estimated by the vector and scalar chiral order parameter within the mean-field approximation are also shown as circles and triangles. The solid square denotes the multi-critical point  $((J/K)_{\text{multi}}, (h/K)_{\text{multi}}) \simeq (11.37, 22.11)$ . The bold line is a guide for the eye.

In the phase diagram, we also mark the phase transition points among the Y-shape, 6-, 12-sublattice and uud phases, which are estimated by the vector and scalar chiral order parameters within the mean-field approximation.

Peculiar properties are expected at the multi-critical point. Since the spin-wave analysis is broken up just at the multi-critical point, we investigate systems close to



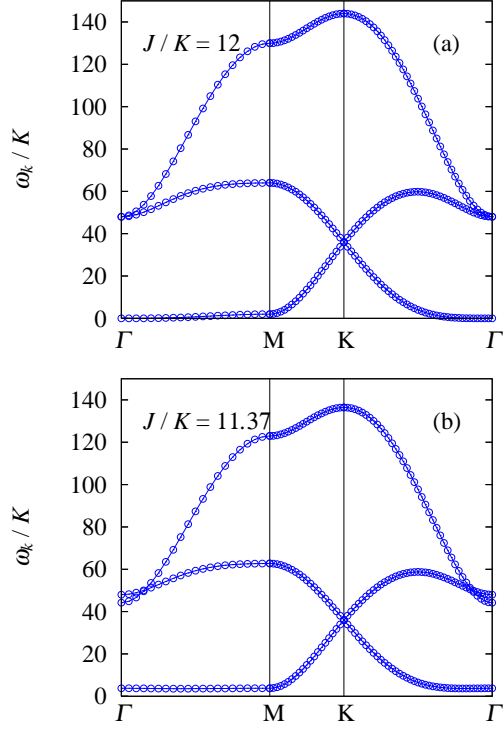


Fig. 9. Three dispersions of the spin wave for (a)  $J/K = 12$  and (b)  $J/K = 11.37 (\simeq (J/K)_{\text{multi}})$  at  $h/K = 24$ . The flat branch is observed along the  $\Gamma$ -M line.

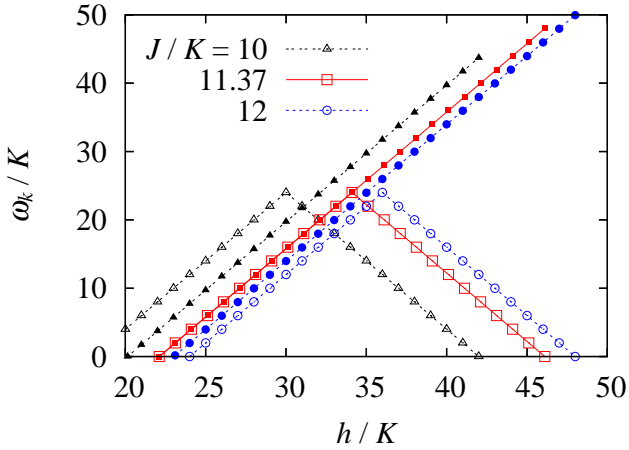


Fig. 10. Magnetic-field dependences of the frequencies of the lowest branch at  $\Gamma$  (open) and M (solid) points for  $J/K = 10, 11.37 (\simeq (J/K)_{\text{multi}})$  and 12. All the lines are guides for the eye.

the point. In Fig. 9 (a) we show the dispersion of the spin wave for  $J = 12K$  and  $h = 24K$  just on the phase-transition line between the Y-shape and the uud phases, which is calculated by the spin-wave theory assuming the uud state as the ground state. We found that the lowest gapless branch has a tendency to be flat along the  $\Gamma$ -M line. Actually, for  $J/K = 11.37 \simeq (J/K)_{\text{multi}}$  the branch along the  $\Gamma$ -M line is flat as shown in Fig. 9 (b). As the magnetic field is increased from the value on the phase-transition line, the frequency of the flat lowest branch for  $J/K = 11.37 \simeq (J/K)_{\text{multi}}$  linearly increases with

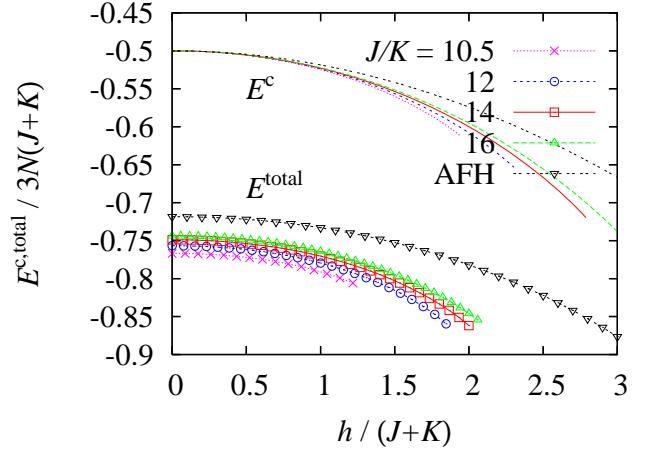


Fig. 11. Magnetic-field dependences of the classical part of the energy  $E^c$  and the total energy  $E^{\text{total}}$  per bond normalized by  $J + K$ . For comparison, the data of the AFH model ( $K = 0$ ) are also shown. The lines on the marks are guides for the eye.

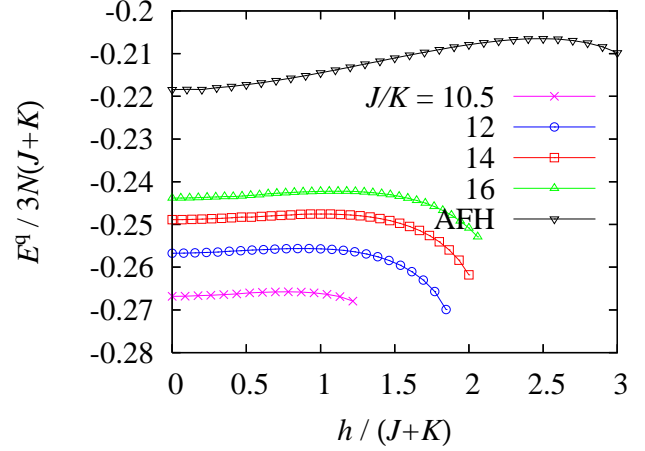


Fig. 12. Magnetic-field dependences of the quantum correction of the energy per bond normalized by  $J + K$ . The lines are guides for the eye.

$h/K$  in the range  $22.11 < h/K \lesssim 34$  as demonstrated in Fig. 10. Since the second branch at the  $\Gamma$  point as shown in Fig. 9 (b) crosses the lowest branch at the  $\Gamma$  point has an inflection at  $h/K \simeq 34$ , the  $h$ -dependence of the frequency of the lowest branch at the  $\Gamma$  point has an inflection at  $h/K \simeq 34$ . When the value of  $J/K$  is shifted from the multi-critical point, the flatness due to the balance of the two- and four-spin exchanges is broken up, though the linearity still holds. In the uud phase the frequency of the lowest branch has the relation  $\omega_k = 2(h - h_1)$  and  $2(h_2 - h)$  for  $h_1 < h < (h_1 + h_2)/2$  and  $(h_1 + h_2)/2 < h < h_2$ , respectively, where  $h_1$  and  $h_2$  are the magnetic fields of the lower and the upper phase boundaries of the uud phase. The linearity of the  $h$ -dependence of the frequency has been also obtained in the uud phase for the quantum AFH model.<sup>22</sup>

## 6. Ground-State Energy and Sublattice Magnetization

The total energy of the ground state is evaluated by  $E^c + E^q$ , where  $E^c$  is the classical energy of Eq. (8) and can be analytically calculated, and  $E^q$  is the quantum energy corresponding to, e.g., Eq. (21) for  $h = 0$ . The magnetic-field dependences of  $E^c$  and  $E^q$  per bonds are shown in Figs. (11) and (12), respectively, where we normalize them by using  $J + K$  to compare with the values of the AFH model. It is found that, as  $J/K$  is decreased, the quantum correction of the energy is increased.

The total magnetization is defined by using the expectation value of the spin  $z$  component, i.e.,

$$M = -\frac{1}{N} \sum_{\text{all } i} \langle \sigma_i^z \rangle. \quad (24)$$

Note that we take the direction of the magnetic field antiparallel to the  $z$  direction. The sublattice magnetizations of the A and B sublattices are defined by

$$m_A = -\frac{3}{N} \sum_{i \in A} \langle \sigma_i^z \rangle = -1 + \Delta m_A, \quad (25)$$

$$m_B = -\frac{3}{N} \sum_{j \in B} \langle \sigma_j^z \rangle = \beta(1 - \Delta m_B), \quad (26)$$

respectively, where from Eqs. (3) and (4),

$$\Delta m_A = \frac{6}{N} \sum_{i \in A} \langle a_i^\dagger a_i \rangle, \quad (27)$$

$$\Delta m_B = \frac{6}{N} \sum_{j \in B} \langle b_j^\dagger b_j \rangle. \quad (28)$$

From a symmetry of the present system, the sublattice magnetization of the C sublattice is same as that of the B sublattice. The total magnetization is written from Eqs. (24)-(26), i.e.,

$$M = M^{\text{cl}} + \Delta M, \quad (29)$$

where

$$M^{\text{cl}} = -\frac{1}{3}(1 - 2\beta), \quad (30)$$

$$\Delta M = \frac{1}{3}(\Delta m_A - 2\beta \Delta m_B). \quad (31)$$

The magnetic-field dependences of  $M$  for various values of  $J/K$  are shown in Fig 13. When  $h = 0$ , the total magnetization is to be zero since the ground state has the  $120^\circ$  structure for all systems. For the AFH system, the value of  $-M$  is increased with  $h$  and saturates to  $-M = 1/3$  at  $h/J = 3$ , where the phase transition to the uud phase occurs. While we can obtain the same behavior as the AFH system for  $J/K = 14$ , the values of  $-M$  become negative for small  $h/(J + K)$  for  $10.5 \leq J/K \leq 12$ . This result shows that the spin-wave theory on the sublattice magnetization is broken up due to strong quantum fluctuations in the region. We also show the  $h$ -dependence of the quantum correction  $\Delta M$  in Fig. 14. The quantum corrections vanish both at  $h = 0$  and the phase transition point to the uud phase.

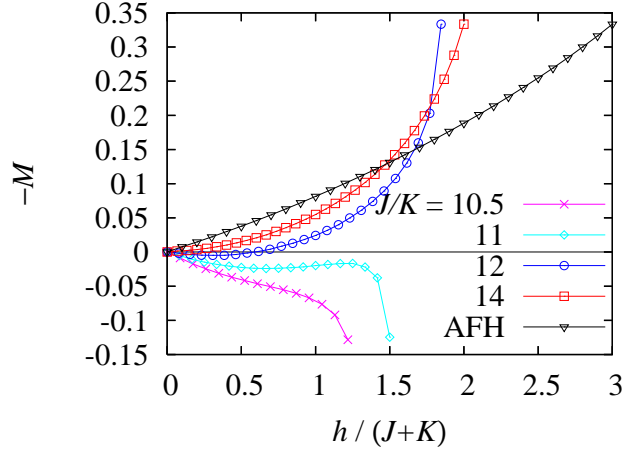


Fig. 13. Dependences of the total magnetization on the magnetic field normalized by  $J + K$ . The data described as AFH are results for  $K = 0$ .

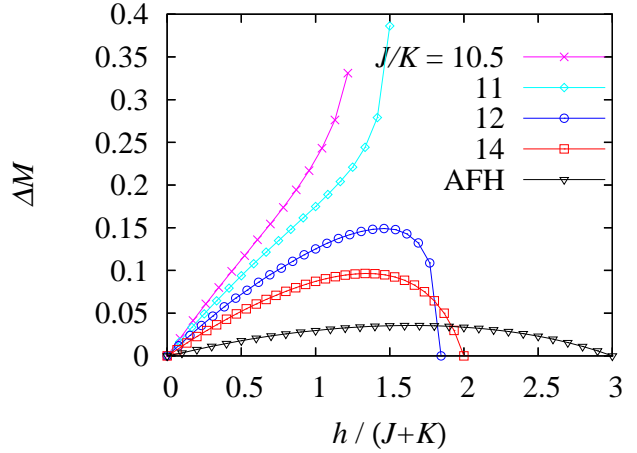


Fig. 14. Dependences of the quantum correction of the total magnetization on the magnetic field normalized by  $J + K$ .

The magnetic-field dependences of the sublattice magnetizations of the A and B sublattices for various values of  $J/K$  are shown in Fig. 15. The values of  $-m_A$  and  $m_B$  are decreased with  $J/K$  and  $h/(J + K)$  except near the phase transition point to the uud phase. The reduction shows that the quantum effects are enhanced by the addition of the four-spin interaction in the MSE model. We also show the dependence of the quantum corrections of the sublattice magnetizations on the magnetic field in Fig. 16. The quantum corrections are larger for smaller  $J/K$  and larger  $h/(J + K)$ . We can obtain an interesting tendency of the size relation between  $\Delta m_A$  and  $\Delta m_B$  within the present spin-wave approximation. In the AFH system with  $K = 0$ , the value of  $\Delta m_A$  is larger than that of  $\Delta m_B$  except for  $h = 0$ . The result suggests that the sublattice magnetization along the axis anti-parallel to the direction of the magnetic field is most sensitive to quantum fluctuation. In the MSE system with the large four-spin interaction and small magnetic field, on the other hand, the sublattice magnetization whose quantization axis tends to parallel to the direction of the mag-

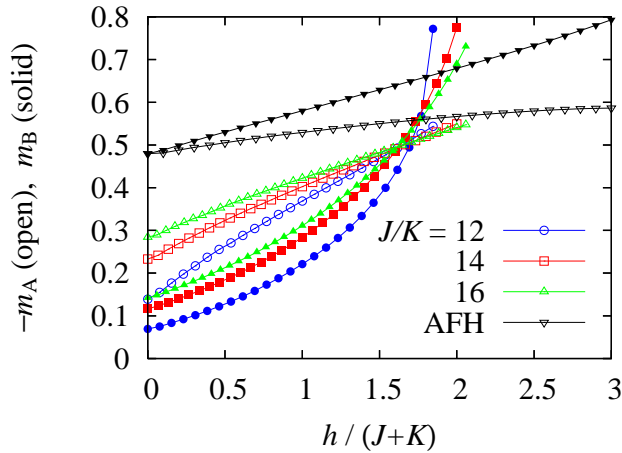


Fig. 15. Dependences of the sublattice magnetizations on the magnetic field normalized by  $J + K$ . The open and solid marks denote  $-m_A$  and  $m_B$ , respectively.

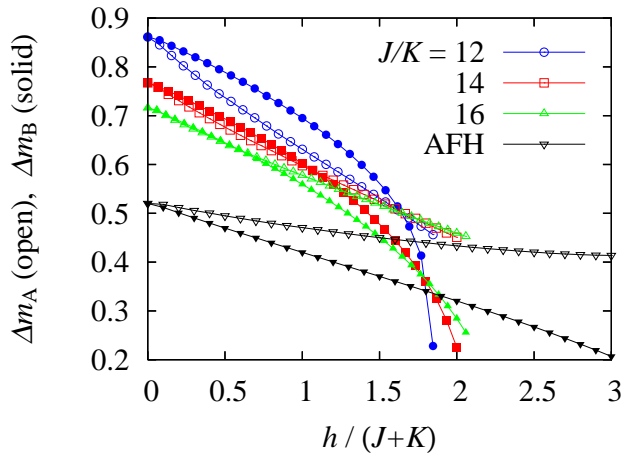


Fig. 16. Dependences of the quantum corrections of the sublattice magnetizations on the magnetic field. The open and solid marks denote  $\Delta m_A$  and  $\Delta m_B$ , respectively.

netic field is most sensitive to quantum fluctuation.

## 7. Summary and Discussions

In the present paper, we studied quantum effects on the 3-sublattice structures in the  $S = 1/2$  multiple-spin exchange model with two-, three- and four-spin exchange interactions on the triangular lattice in the magnetic field. By using the linear spin-wave theory, we found that the coplanar Y-shape state is stable as the ground state of the quantum system, though the four-spin interaction leads to the instability as the softening of the spin wave and the phase transition to the 6-sublattice phase occurs.

We had arguments in the framework of the linear spin-wave theory. Within the approximation, the magnetization becomes negative in the parameter region where the four-spin exchange interaction is dominant. We should take into account higher-order corrections of the spin

wave to estimate the magnetization in the region.

The exact diagonalization study of finite clusters predicted that the ground state is a spin-liquid state with a spin gap filled with a large number of singlet states for parameters corresponding to our 6-sublattice phase.<sup>23</sup> The character of the ground state in this parameter region is, however, still not clarified. In order to numerically examine the possibility of the 6-sublattice phase, we would need the exact diagonalization of clusters with larger sizes. The spin-wave analysis assuming the 6-sublattice structure as the ground state is another interesting problem remained for the future work.

## Acknowledgements

We acknowledge useful discussions with Y. Uchihira. This work is partly supported by Grants-in-Aid for Scientific Research Programs (No. 17071011, No. 17540339, No. 18740239) and 21st Century COE program from the Ministry of Education, Culture, Sports, Science and Technology of Japan.

- 1) H. Franco, R. E. Rapp and H. Godfrin, Phys. Rev. Lett. **57** (1986) 1161.
- 2) H. Godfrin, R. R. Ruel and D. D. Osheroff, Phys. Rev. Lett. **60** (1988) 305.
- 3) M. Siqueira, J. Nyéki, B. Cowan and J. Saunders, Phys. Rev. Lett. **76** (1996) 1884.
- 4) K. Ishida, M. Morishita, K. Yawata and H. Fukuyama, Phys. Rev. Lett. **79** (1997) 3451.
- 5) K. Kubo and T. Momoi, Z. Phys. B **103** (1997) 485.
- 6) T. Momoi, K. Kubo and K. Niki, Phys. Rev. Lett. **79** (1997) 2081.
- 7) K. Kubo, H. Sakamoto, T. Momoi and K. Niki, J. Low Temp. Phys. **111** (1998) 583.
- 8) G. Misguich, B. Bernu, C. Lhuillier, J. Low Temp. Phys. **110** (1998) 327.
- 9) G. Misguich, B. Bernu, C. Lhuillier and C. Waldtmann, Phys. Rev. Lett. **81** (1998) 1098.
- 10) G. Misguich, C. Lhuillier, B. Bernu and C. Waldtmann, Phys. Rev. B **60** (1999) 1064.
- 11) M. Roger, C. Bäuerle, Yu. M. Bunkov, A.-S. Chen and H. Godfrin, Phys. Rev. Lett. **80** (1998) 1308.
- 12) T. Momoi, H. Sakamoto and K. Kubo, Phys. Rev. B **59** (1999) 9491.
- 13) K. Kubo and T. Momoi, Physica B **329-333** (2003) 142.
- 14) R. Masutomi, Y. Karaki and H. Ishimoto, Phys. Rev. Lett. **92** (2004) 025301.
- 15) Y. Kurosaki, Y. Shimizu, K. Miyagawa, K. Kanoda and G. Saito, Phys. Rev. Lett. **95** (2005) 177001.
- 16) D. J. Thouless, Proc. Phys. Soc. (London) **86** (1965) 893.
- 17) It was called umbrella state in ref. 5.
- 18) H. Kawamura and S. Miyashita, J. Phys. Soc. Jpn. **54** (1985) 4530.
- 19) B. Bernu and D. Ceperley, in *Quantum Monte Carlo Methods in Physics and Chemistry*, edited by M. P. Nightingale and C. J. Umrigar (Kluwer, Dordrecht, The Netherlands, 1999).
- 20) T. Holstein and H. Primakoff, Phys. Rev. **58** (1940) 1098.
- 21) J. H. P. Colpa, Physica **93A** (1978) 327.
- 22) A. V. Chubukov and D. I. Golosov, J. Phys.: Condens. Matter **3** (1991) 69.
- 23) W. LiMing, G. Misguich, P. Sindzingre and C. Lhuillier, Phys. Rev. B **62** (2000) 6372.